View metadata, citation and similar papers at core.ac.uk
brought to you by CORE
provided by CERN Document Server

EUROPEAN ORGANIZATION FOR NUCLEAR RESEARCH

CERN/PPE 96-128
20 September 1996

Observation of vertex factorisation breaking in central pp interactions

The WA91 Collaboration

D. Barberis[5], W. Beusch[5], F.G. Binon[7], J.N. Carney[4], D. Di Bari[3], A.V. Dolgopolov[9], S.V. Donskov[9], B.C. Earl[4], D. Elia[3], D. Evans[4], R. Fini[3], B.R. French[5], B. Ghidini[3], S. Inaba[11], A.V. Inyakin[9], A. Jacholkowski[5], G.V. Khaustov[9], T. Kinashi[10], J.B. Kinson[4], A. Kirk[4], W. Klempt[5], M. Kobayashi[11], A.A. Kondashov[9], Y. Kulchitsky[6], A.A. Lednev[9], V. Lenti[3], V.A. Lishin[9], R.A. Loconsole[3], S. Maljukov[6], V. Manzari[3], P. Martinengo[5], I. Minashvili[6], T. Nakagawa[12], F. Navach[3], K.L. Norman[4], J.P. Peigneux[1], S.A. Polovnikov[9], V.A. Polyakov[9], Yu.D. Prokoshkin[9], V. Romanovsky[6], H. Rotscheidt[5], N. Russakovich[6], V.D. Samoylenko[9], A. Semenov[6], M. Sené[5], R. Sené[5], P.M. Shagin[9], H. Shimizu[8], A.V. Shtannikov[9], A.V. Singovsky[9], A. Solovjev[6], J.P. Stroot[7], V.P. Sugonyaev[9], K. Takamatsu[8], G. Tchlatchidze[6], T. Tsuru[11], G. Vassiliadis[2], M. Venables[4], O. Villalobos Baillie[4], M.F. Votruba[4], Y. Yasu[11]

Abstract

Central $\pi^+\pi^-$ events produced in pp interactions are studied in terms of correlations between the outgoing protons. It is observed there is more $\rho^0(770)$ and $f_2(1270)$ production in reactions where the outgoing protons are on opposite sides of the beam. This effect is not attributable to the trigger or the experimental acceptance, and suggests that the vertices do not factorise.

Dedicated to the memory of our colleague and friend Georges Vassiliadis

Submitted to Physics Letters

1 LAPP-IN2P3, Annecy, France.
2 Athens University, Nuclear Physics Department, Athens, Greece.
3 Dipartimento di Fisica dell'Università and Sezione INFN, Bari, Italy.
4 School of Physics and Space Research, University of Birmingham, Birmingham, U.K.
5 CERN - European Organization for Nuclear Research, Geneva, Switzerland.

6 JINR, Dubna, Russia.
7 IISN, Belgium.
8 Faculty of Engineering, Miyazaki University, Miyazaki, Japan.
9 IHEP, Protvino, Russia.
10 RCNP, Osaka University, Osaka, Japan.
11 KEK, Tsukuba, Japan.
12 Faculty of Science, Tokohu University, Sendai, Japan.
13 Faculty of Science, Yamagata University, Yamagata, Japan.

The WA91 experiment is designed to study exclusive final states formed in the reaction

$$\mathrm{pp} \longrightarrow \mathrm{p}_f X^0 \mathrm{p}_s,$$

where the subscripts f and s refer to the fastest and slowest protons in the laboratory frame respectively and X^0 represents the centrally produced system. Reactions of this type are expected to be mediated by double exchange processes, with a mixture of Pomeron-Pomeron, Reggeon-Pomeron and Reggeon-Reggeon exchange.

The WA76 experiment [1] observed that in the $\pi^+\pi^-$ channel the ratio of the cross-sections for the production of $\rho^0(770)$ at centre-of-mass energies $\sqrt{s} = 23.8$ GeV and $\sqrt{s} = 12.7$ GeV respectively was 0.44 ± 0.07. Furthermore, WA76 also reported that $\rho^0(770)$ production is enhanced at high four-momentum transfer, $|t|$. Since Double Pomeron Exchange (DPE) cannot produce $I = 1$ states such as the $\rho^0(770)$, these observations suggest that DPE becomes relatively more important at low $|t|$ and high $\sqrt{s}$, in agreement with theoretical expectations [2]. In DPE, factorisation of the two vertices would lead us to expect no correlation between the resonances seen in the $\pi^+\pi^-$ mass spectrum and the azimuthal angle between the outgoing protons.

In this letter we present a study of centrally produced meson systems, using data from the 1994 run of the WA91 experiment, in terms of the directions taken by the outgoing fast and slow protons. The data were taken at an incident beam momentum of 450 GeV/c, equivalent to $\sqrt{s} = 28$ GeV. The layout of the Omega Spectrometer used in this run is shown in figure 1 and comprises:

1. A set of detectors to perform an accurate measurement of the incident beam direction. This was achieved using a telescope of ten 20 μm pitch microstrip detectors ($5y$ and $5z$ planes).

2. A 60 cm long hydrogen target and a system of scintillator hodoscopes for the trigger definition (as described below).

3. Fifteen 2 mm pitch (A and B) Multi-Wire Proportional Chambers (MWPCs), one 1 mm pitch MWPC and two Drift Chambers (DC) to measure the medium momentum charged tracks.

4. Sixteen (eight left and eight right) 2 mm pitch (C) MWPCs to measure the slow proton.

5. A system of microstrip detectors placed in two stations 5 m and 10 m downstream of the centre of Omega in order to measure the outgoing fast track, which was typically in the momentum range 350-450 GeV/c.

6. Two threshold Čerenkov detectors, Č1 and Č2, and three scintillator hodoscopes, HY1, HY2 and HY3, used for charged particle identification.

7. The GAMS-4000 electromagnetic calorimeter used for the energy and coordinate measurement of photons.

The trigger required:

1. A fast particle crossing the downstream microstrip telescope. This requirement was fulfilled by asking for a coincidence between two scintillation counters (A1 and A2) placed close to the microstrip detectors at 5 m and 10 m. A2 was split vertically into two 2.5 cm $\times$ 5 cm elements, A2L and A2R, in order to determine the y-direction, in the Omega coordinate system, taken by the fast track.

2. A slow particle left [right] was defined by requiring one hit on any of the fourteen slabs of the Slow Proton Counter Left (SPC(L)) [Right (SPC(R))] in coincidence with a hit in the left [right] elements of the box counter (TB) and at least one hit in each of two planes of the C MWPCs on the left [right] side of the target.

3. In order to reduce backward diffraction or excitation events, zero hits were required in the other three sides of TB, which was left open at its front end so that the fast track and centrally produced particles did not veto the event.

After selecting the slow and fast particles, the major background to centrally produced events is elastic scattering. When the slow and fast particles are on the same side of the beam, *i.e.*, a slow left proton and a hit in A2(L) (classified as LL), or a slow right proton and a hit in A2(R) (RR), elastically scattered events are excluded by momentum conservation. For the combinations slow proton left and A2(R) (classified as LR) or slow proton right and A2(L) (RL), the number of elastic scattering events triggered on were reduced by requiring that at least one hit be detected in the downstream hodoscope HY1. Reactions of the type

$$\mathrm{pp} \longrightarrow \mathrm{p}_f \ (\pi^+\pi^-) \ \mathrm{p}_s \ ,$$

were selected from the sample of four-prong events by requiring

$$\begin{aligned} |\text{missing } p_x| &< 14.0 \text{ GeV}/c, \\ |\text{missing } p_y| &< 0.16 \text{ GeV}/c, \\ |\text{missing } p_z| &< 0.08 \text{ GeV}/c. \end{aligned}$$

In addition, the Ehrlich Mass squared, m_X^2 [3], defined by

$$m_X^2 = \frac{[(E_b+m_\mathrm{p}-E_{\mathrm{p}_f}-E_{\mathrm{p}_s})^2-p^2_{\pi^+}-p^2_{\pi^-}]^2-4p^2_{\pi^+}p^2_{\pi^-}}{4(E_b+m_\mathrm{p}-E_{\mathrm{p}_f}-E_{\mathrm{p}_s})^2},$$

was required to be in the range

$$-0.3 \text{ GeV}^2 < m_X^2 \leq 0.16 \text{ GeV}^2,$$

and finally the principal diffractive production channels in the pπ spectra were removed by requiring

$$m_{\mathrm{p}\pi} > 1.5 \text{ GeV},$$

where $m_{\mathrm{p}\pi}$ represents the mass of the pπ system.

Although the hardware trigger vetoes most of the elastic events, it does not uniquely define events which have a fast track with $p_y > 0$ or $p_y < 0$, since fast right tracks with low p_y bend in the magnetic field so that they sometimes hit A2(L) instead of A2(R). In order to remove bias caused by this effect, we do not use the hardware trigger condition in the analysis to define the direction taken by the fast track. Instead, we define a fast left proton as being one which has a positive p_y relative to the beam, and a fast right proton as being one which has a negative p_y relative to the beam. As mentioned above, RL and LR triggers have an extra constraint imposed on them in order to reduce the elastic background, namely at least one hit must be detected in the downstream hodoscope HY1. In order to ensure that the same conditions apply to all trigger types, we require that both pions trace to the hodoscope plane for all events. In figure 2 the $\pi^+\pi^-$ mass is plotted as a function of trigger type. Large enhancements of the $\rho^0(770)$ and $f_2(1270)$ signals are observed in the RL and LR cases.

Since we have higher statistics for triggers with a slow left proton than for triggers with a slow right proton, and also since slow left protons are generally better reconstructed, in the following analysis we concentrate on events with a slow left trigger. However, events with a slow right proton show similar effects to those with a slow left proton.

In light of the WA76 observation [4] that the amount of $\rho^0(770)$ production varies with the 4-momentum transfer at the vertices, it is important to check whether LL triggers favour low $|t|$ or LR triggers favour high $|t|$. In order to do this, we first generate a set of Monte Carlo data under the assumption that there is no correlation between the fast and slow vertices. The Monte Carlo data are tested to see if they pass through the geometrical acceptance of the detectors, and from this a set of corrections for the $|t|$ distributions of the real data is produced. We choose data in two mass ranges, $0.7 < m_{\pi^+\pi^-} \leq 0.9$ GeV and $1.1 < m_{\pi^+\pi^-} \leq 1.4$ GeV, corresponding to the $\rho^0(770)$ and $f_2(1270)$ masses regions. The efficiency corrected distributions, fitted to the form $Ae^{-\alpha|t|}$, are shown in figure 3. The values of the slope parameter α for a maximum likelihood fit in the region $0.1\ \text{GeV}^2 < |t| \leq 0.6\ \text{GeV}^2$ for the $\rho^0(770)$ mass region and $0.1\ \text{GeV}^2 < |t| \leq 0.45\ \text{GeV}^2$ for the $f_2(1270)$ region are given in table 1, where the errors are statistical only. The values of the t slopes for LL and LR data within one mass region are similar, although we do observe some variation of the $|t|$ slopes with mass, since the slopes for the $f_2(1270)$ mass region are rather shallower than those for the $\rho^0(770)$ region. In summary, the differences in the resonances observed in the $\pi^+\pi^-$ mass spectra for the LL and LR triggers are not due to a difference in acceptance in $|t|$ for the two triggers.

Shown in figure 4 are mass spectra for K^+K^- and $\pi^+\pi^-\pi^+\pi^-$ taken during the same run. The K^+K^- mass spectra are shown in figures 4 *a* and *b*. The $f_2'(1525)$ is a well known $q\overline{q}$ state, and is seen with a considerably stronger signal in the LR case. Interestingly, the $\theta/f_J(1710)$ signal in K^+K^- is stronger in the LL mass spectrum. The $\pi^+\pi^-\pi^+\pi^-$ mass spectra shown in figures 4 *c* and *d* show a clear enhancement of the $q\overline{q}$ state $f_1(1285)$ in LR triggers.

The SFM Collaboration also observed that the directions taken by the outgoing fastest and slowest particles in central interactions are correlated with the centrally produced states [5]. They see an enhancement of $f_2(1270)$ production in the $\pi^+\pi^-$ channel in cases where the fastest and slowest particles in the laboratory frame have a "back-to-back" configuration of their momenta. This is consistent with the enhancement of $f_2(1270)$ production in the WA91 data in LR and RL triggers. However, the SFM Collaboration concluded that this may suggest that the $f_2(1270)$ has a large glueball content. This certainly does not seem consistent with

the WA91 observation that there is also an enhancement of the $\rho^0(770)$ signal in LR and RL triggers, since the $\rho^0(770)$ is well understood as having only a quark-like, not a glueball, nature.

In conclusion, we have studied the centrally produced $\pi^+\pi^-$ system in pp interactions at a beam momentum of 450 GeV/c. A strong correlation is observed between the directions of the outgoing protons and the strength of the $\rho^0(770)$ and $f_2(1270)$ signals. Specifically, in situations where the outgoing protons are on opposite sides of the beam (LR and RL), more $\rho^0(770)$ and $f_2(1270)$ are produced than in cases where the protons are in the same hemisphere (LL and RR). This is not attributable to trigger or acceptance effects. A study of the K^+K^- channel shows a significant enhancement in the amount of $f_2'(1525)$ production in the LR and RL triggers, but the $\theta/f_J(1710)$ is seen predominantly in the LL and RR triggers. In the $\pi^+\pi^-\pi^+\pi^-$ channel, the $f_1(1285)$ is seen to be enhanced in the LR and RL channels. These observations are in in disagreement with simple models of double exchange mechanisms, where the exchange vertices are assumed to factorise and hence be uncorrelated.

References

[1] T.A. Armstrong et al., Phys. Lett. **B 227** (1989) 186.

[2] S.N. Ganguli and D.P. Roy, Phys. Rep. **67** (1980) 203.

[3] R. Ehrlich et al., Phys. Rev. Lett. **20** (1968) 686.

[4] T.A. Armstrong et al., Z. Phys. **C 51** (1991) 351.

[5] A. Breakstone et al., Z. Phys. **C 48** (1990) 569.

Figure Captions

Figure 1 : WA91 1994 experimental layout

Figure 2 : $\pi^+\pi^-$ mass spectra for a) LL, b) LR, c) RR and d) RL for events where both π tracks reach HY1

Figure 3 : Acceptance corrected $|t_f|$ and $|t_s|$ distributions for a) LL and b) LR in the $\rho^0(770)$ mass region, and c) LL and d) LR for the $f_2(1270)$ mass region

Figure 4 : Mass spectra for K^+K^- a) LL, b) LR, and for $\pi^+\pi^-\pi^+\pi^-$ c) LL, d) LR

Table 1: Values of the slope parameter α for acceptance corrected data

Trigger	$\alpha_{\rho^0(770)}$ / GeV^{-2}	$\alpha_{f_2(1270)}$ / GeV^{-2}
LL $\lvert t_f \rvert$	8.0±0.1	6.0±0.2
LL $\lvert t_s \rvert$	8.0±0.1	5.4±0.2
LR $\lvert t_f \rvert$	7.3±0.1	6.0±0.2
LR $\lvert t_s \rvert$	7.4±0.1	5.6±0.2

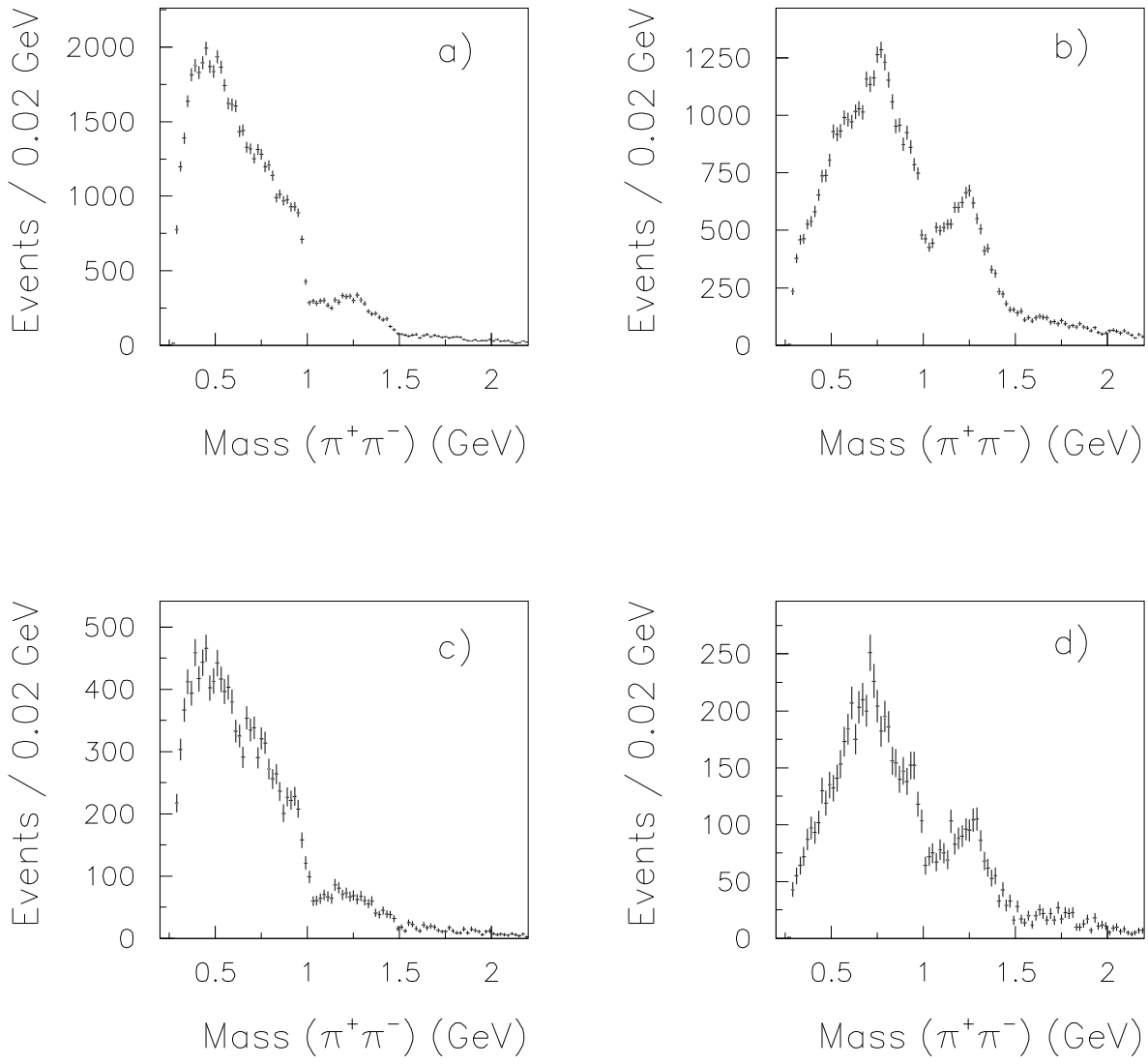
a)
b)
c)
d)
Events / 0.02 GeV
Mass $(\pi^+\pi^-)$ (GeV)
0
500
1000
1500
2000
250
750
1250
100
200
300
400
50
150
0.5
1
1.5
2

Figure 2:

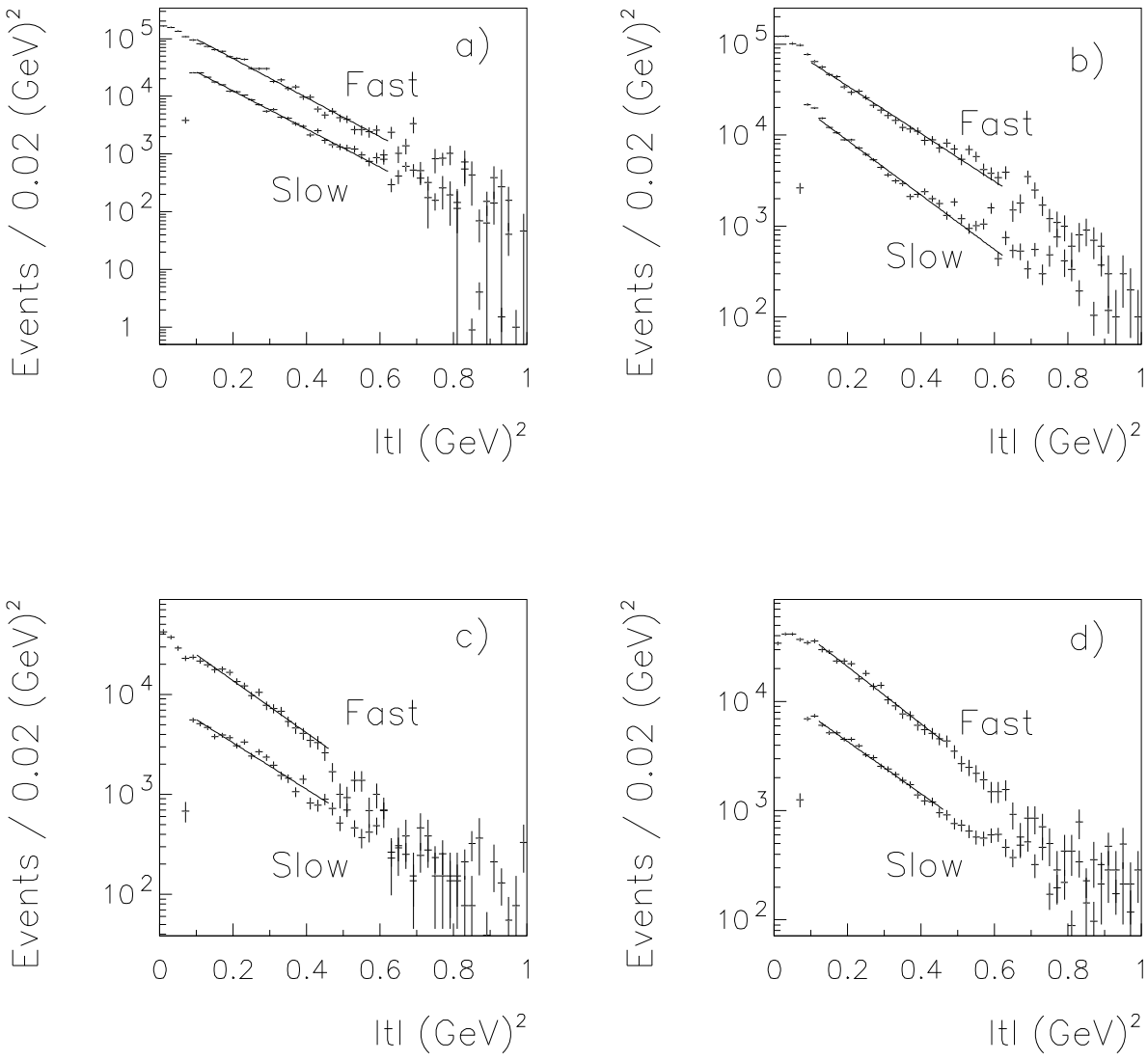

Figure 3:

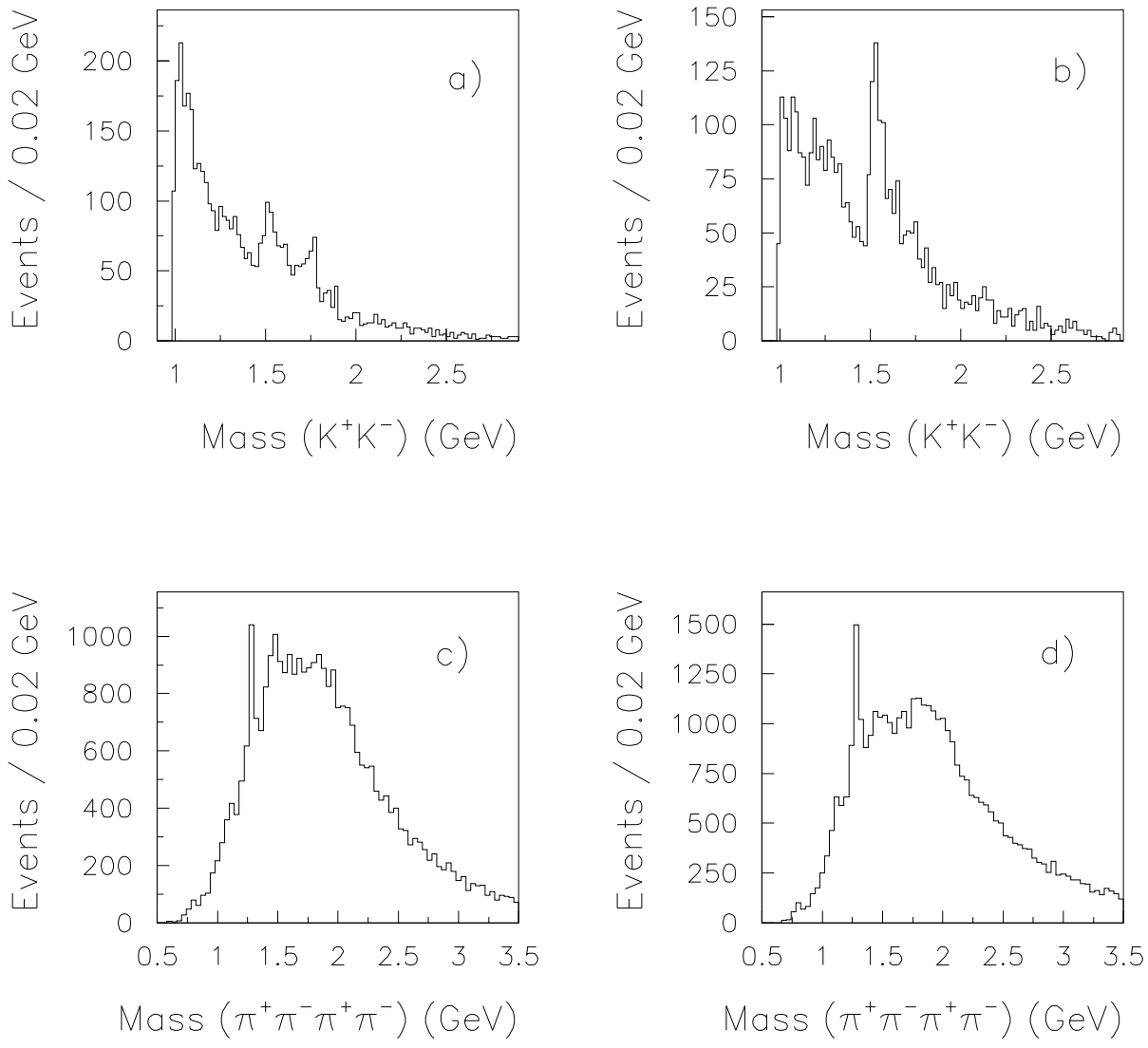
Events / 0.02 GeV
a)
Mass (K^+K^-) (GeV)
b)
Mass (K^+K^-) (GeV)
c)
Mass $(\pi^+\pi^-\pi^+\pi^-)$ (GeV)
d)
Mass $(\pi^+\pi^-\pi^+\pi^-)$ (GeV)

Figure 4: